THE DEPTH DISTRIBUTION OF DISPLACEMENT DAMAGE IN α-IRON UNDER "TRIPLE BEAM" ION IRRADIATION*

L. L. Horton,[1] J. Bentley,[2] and W. A. Jesser[1]
[1]Department of Materials Science, University of Virginia, Charlottesville, VA 22901
[2]REMAG, Oak Ridge National Laboratory, Oak Ridge, TN 37830

The depth dependence of the defect structures was determined for iron irradiated at 850 K with 4 MeV Fe^{++} and energetic helium and deuterium ions to 10 dpa and fusion levels of helium and deuterium. From the damage profiles, a sectioning depth of 0.9 μm was selected for studies of iron and bcc iron alloys, such as ferritic steels, utilizing similar irradiation parameters. A comparison of the experimental damage profile to the deposited energy and deposited ion profiles calculated by E-DEP-1 indicated a possible overestimate of the LSS stopping power of at least 22%.

1. INTRODUCTION

Ferritic stainless steels are currently being considered as structural materials for first wall and blanket applications for proposed fusion reactors. Therefore, characterization of the defect structures which result from fusion environment radiation damage of these steels is of interest. One technique commonly used to study the development of microstructural radiation damage utilizes energetic ion irradiations. The "triple-beam" ion irradiation procedure developed at ORNL is particularly applicable to fusion studies [1-3]. In this type of irradiation, energetic heavy ions, helium ions and deuterium ions simultaneously bombard the specimens. The heavy ions create atomic displacements. The helium and deuterium ions are injected so as to come to rest within the damaged region and simulate transmutation-produced helium and hydrogen.

In triple-beam irradiations, as in most ion irradiations, the damaged region is usually within a few micrometers of the irradiated surface. The defect structures vary significantly with distance from the irradiated surface. Simple "back-thinning" from the unirradiated surface of the specimen would limit 120 kV transmission electron microscope (TEM) examinations to the region within about 250 nm of the irradiated surface. In this region, surface effects would dominate the observations. Therefore, controlled removal or "sectioning" of the damaged region is necessary prior to back-thinning for preparation of TEM specimens. The sectioning depth can best be selected by experimentally determining the depth distribution of defect structures.

Three experimental methods are commonly used to determine defect profiles. In the first, the ion-irradiated specimen is back-thinned and the defect distribution determined from stereo, HVEM, micrographs. The second technique utilizes sectioning of specimens to various depths followed by back-thinning and TEM examination. The final method is TEM examination of a cross-sectional area of a bombarded foil. In order to bring the damaged region to the center of the TEM disk, the cross-sectional area of the foil is increased by electroplating or sputter deposition. The cross-section technique was first used by Spurling and Rhodes [4] in 1972. Since then, this basic technique has been used by a number of investigators to study damage profiles in stainless steel [4,5], nickel [6-13], copper [14-16], and molybdenum [17].

Relatively few studies of the effect of gas implantation on the heavy ion damage profile have been reported. Two investigations have reported profiles for simultaneous bombardment by heavy ions and gas ions. These studies on molybdenum [17] and nickel [12,13] utilized a dual beam of energetic Ni^{++} and He^{+} ions. No damage profiles for triple-beam irradiated materials are reported. The only damage profiles for a ferritic material are those of Kuramoto et al. [18] for single 4 MeV Ni^{++} ion bombardment of pure iron. For the current study, the depth distribution of the defect structures in triple-beam ion-irradiated iron was determined using the electroplating, cross-sectional area technique. Iron was selected because of its importance as the basis of ferritic steels. The sectioning depth determined from the damage distribution in iron has been used in a detailed study of the microstructures in triple-beam irradiated Fe-Cr alloys [19]. This information is also expected to be applicable to studies utilizing triple-beam irradiation of ferritic steels.

2. EXPERIMENTAL PROCEDURE

Disk specimens of α-iron (34 wt ppm C) (3 mm in diameter) were bombarded to 10 dpa, 100 at. ppm He and 410 at. ppm D with a triple beam of He^{+}, D_2^{+}, and 4 MeV Fe^{++} at 850 K in the dual Van de Graaff accelerator system at ORNL [1-3]. These are the helium and deuterium (hydrogen) concentration to dpa ratios expected to develop in a

*Research sponsored by the U.S. Department of Energy; by the Division of Materials Sciences, under contract No. W-7405-eng-26 with Union Carbide Corporation, and by the Office of Fusion Energy under a contract with the University of Virginia.

ferritic steel first wall [20,21]. Details concerning the specimen preparation can be found in ref. [19]. The energy of the He^+ and D^+ beam was ramped sinusoidally at 2.5×10^{-2} Hz between 0.2 and 0.4 MeV. This insured that the helium and deuterium were implanted over the heavy ion damage region with profiles similar to those shown in Fig. 1. The shape of the light ion profile was assumed to be the same as those experimentally determined for nickel and stainless steel targets [1]. The depth of the profiles was determined from tabulated values for the ion ranges [22,23]. These values are calculated from the stopping powers of helium and deuterium in iron, which, in the energy range of interest, are not well known. The few experimental values reported have differences of up to 20% for helium and 10% for deuterium, indicating that a significant error in the ion range is possible.

The irradiated specimens were electroplated at 370 to 372 K in a ferrous chloride plating bath. Calcium chloride was added to the plating bath at a ratio of 1 part $CaCl_2$ to 2.6 parts $FeCl_2$. The pH of the bath was maintained between 0.15 and 1.5 with additions of small amounts of hydrochloric acid. The bath was agitated constantly during the plating by a magnetic stirrer. A FerroVac-E iron anode was used. The current density for the plating was 1 to 10 kA/m^2. About 4 to 5 mm of iron were plated onto the original specimen in two to three days. Three or four wafers 0.3 mm thick were cut from each electroplated specimen with slices normal to the original, irradiated surface. A single 3-mm-dia disk specimen was electrodischarge machined from each wafer. Final electropolishing was performed in a TENUPOL jet electropolishing apparatus. Electron-transparent area was obtained at the

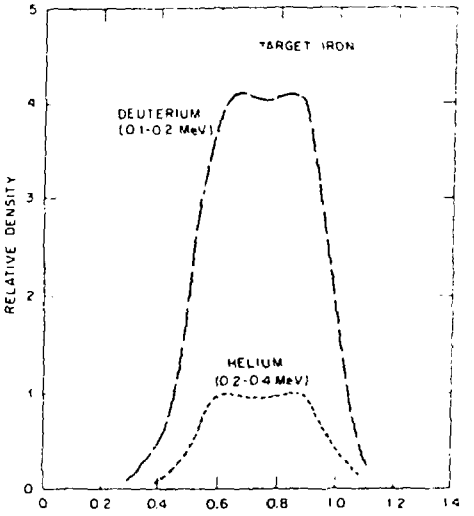

Fig. 1. Calculated helium and deuterium profiles for an iron target.

irradiated surface-electroplate interface in about 30% of the specimens.

The specimens were examined in a JEM 120C TEM equipped with a special objective lens polepiece (AMC) for the observation of magnetic materials [24]. This pole-piece allows high-angle tilting experiments, such as dislocation loop analyses, to be performed.

3. RESULTS

All aspects of the results described below were observed in multiple areas in each of several specimens. In general, the damage microstructures consisted of both dislocations and cavities. The microstructural distributions varied with distance from the irradiated surface electroplate interface. There was a zone denuded of cavities from the interface to 0.1 μm, a typical observation in ion damage profiles. The observed depth distribution is summarized in Fig. 2. Figure 2 allows direct comparison of the micrograph of the damage profile and the measured quantitative data for the dislocation density and cavity parameter profiles. The data were measured for each of seventeen 0.2 μm wide regions covering the entire width of the damage profile. The values obtained for each region are plotted in Fig. 2 at the midpoint of the region.

The cavities had a crystallographic shape. The diameter of the cavities was measured assuming a spherical cavity with a circular projection of the same area as the projected crystallographic shape. The cavity volume fraction or swelling was calculated from the volume average cavity diameter and the cavity concentration. The swelling is plotted in Fig. 2 with the cavity parameters. The swelling was a maximum of about 0.22% over a range of depths from 0.9 to 1.1 μm from the interface.

The major form of the dislocation microstructure was a coarse network. A few dislocation loops appear with the network in the distribution at 1.6 to 2.2 μm from the interface. A higher concentration of loops is present within a discrete band extending from 2.4 to 3.4 μm from the interface. The loops in both regions were analyzed using the method of Maher and Eyre [25]. The loops were determined to be interstitial in nature with predominantly a⟨100⟩ Burgers vectors. A few a/2⟨111⟩ Burgers vectors were also observed in each of the two loop regions.

4. DISCUSSION

The qualitative appearance of the damage profiles observed in the current investigation agree with those reported for dual ion irradiation of other materials. In order to select a sectioning depth, the profiles were compared to the deposited energy and ion depth profiles for a MeV Fe^{++} ion bombardment of iron shown in Fig. 3. These profiles were calculated using the E-DEP-1 computer code of Manning and Mueller [26]. This

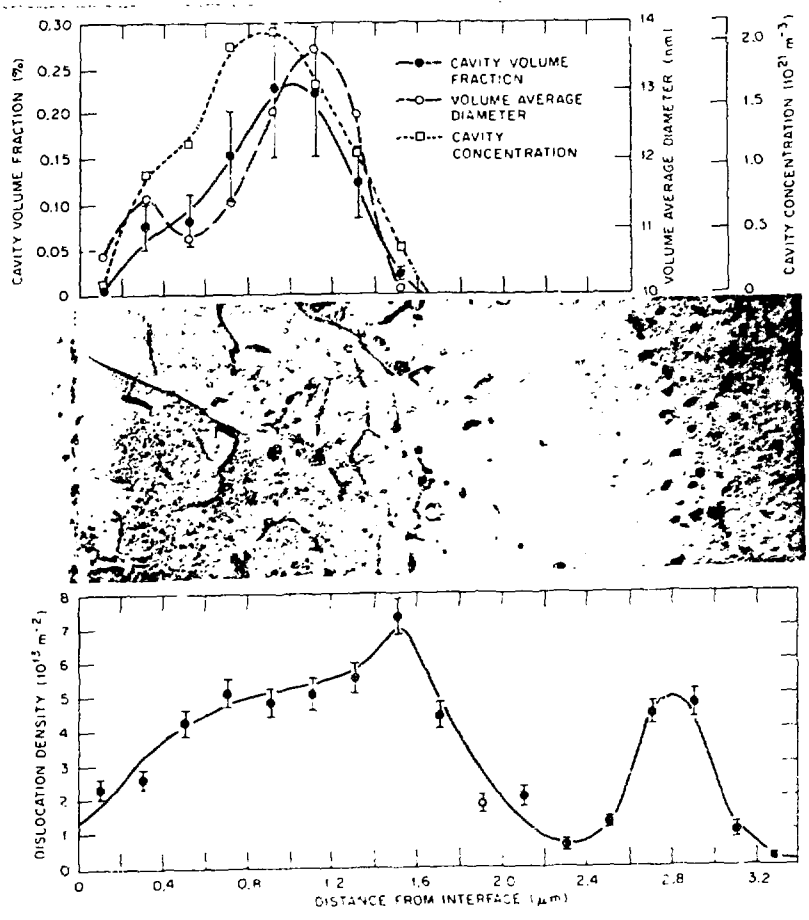

Fig. 2. The damage profiles for triple-beam ion-irradiated iron. The distances from the interface indicated on the horizontal axis at the bottom of the figure applies to the micrograph, the dislocation density profile, and the cavity parameter profiles.

code used the theoretical stopping power, k, of 0.15% as calculated by the Lindhard, Scharff, and Schiott (LSS) theory.

4.1 Swelling Profiles

A comparison of Fig. 3 with the experimentally obtained profiles, Fig. 2, indicates that the peak swelling corresponds to the peak of deposited ions rather than the expected correspondence with the peak in the deposited energy. As also shown in Fig. 3, if the value for k is reduced by 22% to 0.121, E-DEP-1 calculates a maximum in the deposited energy at 1.0 μm, the location of the observed swelling peak. The possibility of an overestimate in the LSS value for k has been suggested by other investigators. Naravan and co-workers have observed that the

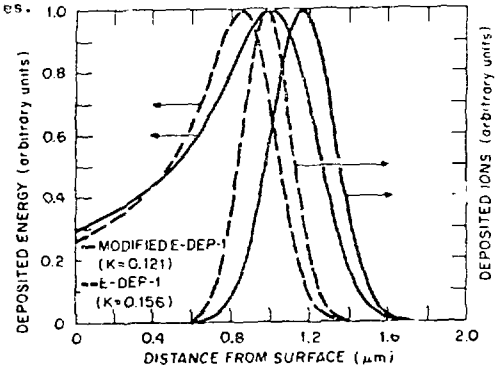

Fig. 3. Deposited energy and deposited ion profiles calculated with E-DEP-1 computer code.

maximum in the point defect density profile was deeper than the maximum of the deposited energy profile predicted by E-DEP-1 for nickel [14] and copper [15] bombarded by 4 MeV nickel ions and for copper bombarded with 5, 16, and 27 MeV copper ions [16]. The calculated depth agreed with the experimental observations if k was reduced. For nickel ion bombardment of nickel, k was reduced by 22%. Narayan and co-workers believe that the lower values of k are related to the oscillations of the electronic stopping when plotted as a function of the target atomic number, z_2. The stopping power has a local minimum at z_2 = 29, and, for 4 MeV energies, is about level between z_2 = 26 and 28. Therefore, the z_2 effect indicates that the percentage of overestimation of k should be about the same for iron and nickel targets. This supports the current observation that a 22% reduction in k for iron leads to agreement between the calculated deposited energy and experimental profiles.

However, the damage profile presented for triple-beam irradiated iron is more complex than the profile for low-dose single-ion irradiations. The cavity profile is affected by many things, including the deposited ions, diffusional spreading, and gas concentration [27]. The deposited interstitials are believed to have the most impact on the location of the swelling peak. In a low swelling material, such as iron, the deposited interstitials will cause the swelling peak to be closer to the irradiated surface than the deposited energy peak. In considering the current swelling profile for iron, the deposited interstitial effect implies that the maximum in the deposited energy profile is even further from the irradiated surface than that calculated for k = 0.121. Calculations by Beeler and Beeler [28] for fcc iron have shown that a value of k = 0.108 is more accurate than the LSS value. Use of this value as input for E-DEP-1 gave the maximum in the deposited energy at 1.06 μm and deposited ions at 1.25 μm (σ = 0.18 μm) from the irradiated surface for bcc iron. Considering the region from 0.9 to 1.6 μm from the surface (±2 σ) of the deposited ion peak, the swelling would be least affected at 0.9 μm, with an increasing effect up to ~ 1.1 μm, where the deposited energy is maximum. This could lead to only slight variations in the swelling profile from 0.9 to 1.1 μm, as observed. The combination of the decreasing deposited energy and the strong interstitial effect could cause the observed rapid decrease in the swelling at depths greater than ~1.1 μm.

Diffusional spreading refers to the migration of point defects to the free surface and to depths beyond the deposited energy profile. The usual manifestation of diffusional spreading is a broadening of the cavity profiles and reduced cavity growth near to the surface. In the current profile, due to the low swelling and strong effect of deposited interstitials, it is unlikely that diffusional spreading would lead to cavity growth beyond the range of the deposited energy from the heavy ions. The effect of the surface on the profile is indicated by the lack of cavities within 0.1 μm of the surface.

The effect of the deposited gas is more difficult to ascertain. For Fe-10% Cr specimens similarly irradiated, the gas has been found to increase the cavity density, decrease the cavity diameter, and increase the swelling [29]. In the damage profile for iron, the slight decrease in the cavity diameter at 0.5 μm could be attributed to the beginning of the implanted gas profile. There is no obvious indication of a similar effect at the end of the implanted gas profile. In fact, the cavity profiles are smooth, suggesting that either the gas is having little effect on the profiles or that any indication of the decreasing gas concentration is masked by the effect of the deposited interstitials and the decreasing damage rate. The latter suggestion implies that the gas concentration levels are approximately the same over the region from 0.9 to 1.1 μm. Further support is provided by the location of the peak cavity concentration within this region. Since the light ion stopping powers, and therefore the ranges, are not very accurately known, as discussed previously, the suggestion that the ions penetrate deeper than indicated in Fig. 1 does not seem unreasonable.

4.2 Dislocation Profiles

Interstitial, edge dislocation loops with $\underline{b} = a\langle 100\rangle$ are commonly observed in iron irradiated at elevated temperatures [30-32]. The formation of interstitial loops with $b = a\langle 100\rangle$ in bcc metals rather than the more energetically favored $a/2\langle 111\rangle$ is accounted for in the model of interstitial loop formation by Eyre and Bullough [33]. Loops with $a\langle 100\rangle$ Burgers vectors are believed to be sessile [32,33].

The presence of dislocations in dual-ion profiles beyond the calculated damage range of the heavy ions is not unusual. Henager et al. [17] have observed dislocation loops at 2 to 3 μm depths in dual ion irradiation (5 MeV Ni and 0.2 MeV He) of molybdenum. The mean damage range of 5 MeV Ni ions in Mo was calculated by E-DEP-1 to be 0.9 μm. The largest loops and the coarsest distribution was found at 2 μm, with the loop diameter decreasing with increasing depth. This behavior can be explained as an effect of the decreasing dose and dose rate within the damage tail coupled with diffusional spreading of the interstitials. At higher displacement levels, i.e., closer to the surface, the loops agglomerated to form a network with a consequent reduction in the dislocation density. In the current profile for iron, this type of loop structure is observed at 1.6 to 2.2 μm. Thus, the discrete band of dislocation loops in iron at 2.4 to 3.4 μm cannot be confused with the observation of Henager et al. This band of dislocation loops is not easily explained. Farrell et al. [13] have observed a discrete band of dislocations

resembling a creep cell wall in nickel irradiated with 4 MeV Ni^{++} and energetically ramped (0.2 to 0.4 MeV)He^{+} ions. They believe that this band is caused by the movement and accumulation of dislocations caused by swelling-induced stresses. In the dislocation band observed in iron, however, the majority of the loops are believed to be sessile. There is no indication that the stress caused by the swelling was sufficient to cause the migration of the network dislocations to this region. It therefore seems unlikely that the stress would be sufficient to cause dislocation loops that nucleated within the major portion of the damage zone to move to the deeper region.

Other possible explanations that have been considered are external stress and energetic extraneous ions. Both of these have been rejected: the former for lack of collaborating observations by other investigators using the same facility for bombardments and the latter due to the absence of an ion of appropriate range within the energy range and the mass selection requirements of the accelerator. Further experiments are under way to characterize the dislocation band more completely.

4.2 Sectioning Depth

Based on the above discussion, a sectioning depth of 0.9 μm was selected. This sectioning depth allows TEM examination of the damage from 0.9 to 1.1 μm from the irradiated surface. In the region extending from 0.80 to 1.2 μm, both the swelling and dislocation density have only small variations in their respective values in the damage profiles. Therefore, the quantitative data obtained from a sectioned specimen would not be adversely affected if the sectioning depth was between 0.85 and 0.95 μm, allowing for small experimental measurement errors.

Acknowledgments

The authors would like to thank M. G. Lewis, Y. K. Chang, H. Harmon, and C. G. McKamey for assistance with the specimen preparation; L. K. Mansur, A. F. Rowcliffe, M. B. Lewis, and K. Farrell for technical comments, and Frances Scarboro for manuscript preparation.

References

[1] Lewis, M. B., IEEE Trans. on Nucl. Sci. Vol. NS-26 (1979) 1320–22.
[2] Farrell, K., Lewis, M. B., and Packan, N. H., Scripta Met. 12 (1978) 1121–24.
[3] Lewis, M. B., Packan, N. H., Wells, G. F., and Buhl, R. A., Nucl. Instr. & Methods, 167 (1979) 233–47.
[4] Spurling, R. A. and Rhodes, C. G., J. Nucl. Mater. 44 (1972) 341–344.
[5] Keefer, D. W. and Pard, A. G., J. Nucl. Mater. 47 (1973) 97–101.
[6] Narayan, J., and Oen, O. S., Proc. of the Workshop on Correlation of Neutron and Charged Particle Damage, CONF-760673 (1976).
[7] Fenske G, Das, S. K., Kaminsky, M., and Miley, G. C., J. Nucl. Mater. 76&77 (1978) 247–248.
[8] Whitley, J. B., Kulcinski, G. L., Wilkes, P. and Smith, H. V., Jr., J. Nucl. Mater. 79 (1979) 159–169.
[9] Fenske, G., Das, S. K., and Kaminsky, M., J. Nucl. Mater. 80 (1979) 373–378.
[10] Fenske, G., Das, S. K., Kaminsky, M., and Miley, G. H., J. Nucl. Mater. 85&86 (1979) 707–711.
[11] Whitley, J. B., Kulcinski, G. L., Wilkes, P., and Billen, J., ibid, pp. 701–706.
[12] Packan, N. H., Farrell, K., and Houston, J. T., 1980 Inter. Metall. Exhibit (ed. by DuBose, C.K.H.) (ASM, Ohio, 1980).
[13] Farrell, K., Packan, N. H., and Houston, J. T., submitted to Radiation Effects.
[14] Narayan, J., Noggle, T. S., and Oen, O. S., in Fundamental Aspects of Radiation Damage in Metals, CONF-751006-P1 (ed. by Robinson, M. T. and Young, F. W., Jr.) (NTIS, Maryland, 1975), pp. 90–97.
[15] Oen, O. S., Narayan, J., and Noggle, T. S., in Application of Ion Beams to Metals (ed. by Picraux, S. T., EerNisse, E. P., and Vook, F. L.) (Plenum Press, New York, 1974), pp. 639–650.
[16] Narayan, J., Oen, O. S., and Noggle, T. S., J. Nucl. Mater. 71 (1977) 169–170.
[17] Henager, C. H., Jr., Brimhall, J. L., and Simonen, E. P., Rad. Effects 36 (1978) 49–55.
[18] Kuramoto, E., Yoshida, N., Tsukuda, N., Kitajima, K., Packan, N. H., Lewis, M. B., and Mansur, L. K., these proceedings.
[19] Horton, L. L., Bentley, J., and Jesser, W. A., included in these proceedings.
[20] Bloom, E. E., J. Nucl. Mater. 85&86 (1979) 795–804.
[21] Gabriel, T. A., Bishop, B. L., and Wiffen, F. W., Nucl. Technol. 38 (1978) 427–433.
[22] Anderson, H. H., and Ziegler, J. F., Hydrogen Stopping Powers and Ranges in All Elements, (Pergamon Press, New York, 1977).
[23] Ziegler, J. F., Helium Stopping Powers and Ranges in All Elements, (Pergamon Press, New York, 1977).
[24] Shimoto, K., Yonezawa, A., Shibatomi, K., and Yanaka, T., Proc. of 34th Annu. EMSA Meeting, (1976), pp. 540–41.
[25] Maher, D. M., and Eyre, B. L., Phil. Mag. 23 (1971) 409–438.
[26] Manning, I., and Mueller, G. P., Comp. Phys. Com. 7 (1974) 85–94.
[27] Mansur, L. K., and Yoo, M. H., J. Nucl. Mater. 85&86 (1979) 523–32.
[28] Beeler, J. R., Jr., and Beeler, M. F., Loc. cit. ref. 15, pp. 651–662.
[29] Horton, L. L., Ph.D. thesis, Department of Materials Science, UVA (1981).
[30] Bentley, J., Horton, L. L., and Farrell, K., 38th Ann. Proc. EMSA (1980), pp. 390–91.
[31] Little, E. A., and Eyre, B. L., AERE-R7095 (March 1972).
[32] Masters, B. C., Phil. Mag. 11 (1965) 881–93.
[33] Eyre, L. L., and Bullough, R., Phil. Mag. 12 (1965) 31–39.
[34] Little, E. A., Rad. Effects 16 (1972) 135–137.